Multi-Color Emission with Orthogonal Input Triggers from a Diarylethene Pyrene-OTHO Organogelator Cocktail

Mark D. Johnstone, Chien-Wei Hsu,[†] Nicolas Hochbaum,[†] Joakim Andréasson* and Henrik Sundén*

Controlling spectral and physicochemical properties with external stimuli is vital for the development of smart materials. Here we demonstrate a supramolecular gelator based on a fluorescent oxotriphenylhexanoate (OTHO) that can switch emission profiles between the solution and gel phase. Furthermore, a cocktail of the gelator and a photochromic diarylethene derivative enables four distinct emissive states to be obtained, which are modulated with light and heat as orthogonal input triggers.

Supramolecular gels[1] resulting from self-assembly of low-molecular-weight gelators (LMWGs) present a robust medium for reversible Sol-Gel transformations that can be controlled by external stimuli, such as heat, ultrasound, and light.[2] By introducing luminescent chromophores to LMWGs, physical transformations are converted into optical signals that can be easily recognized by the naked eye.[3] For example, aggregation induced emission (AIE) chromophores can provide an optical signal depending on the physical state, as the gelator shows intense emission in gel state while weak emission in solution.[4] In addition to AIE, the emission color can also be changed by modulating intermolecular exited-state aromatic interactions, such as excimer formation,[5] typically resulting in emission at longer wavelengths. As such, photophysical phenomena can be used to provide *in situ* information on the molecular packing of the gels, complementary to infrared and NMR spectroscopic techniques.[6] For example, Kato and co-workers reported a pyrene-based gel in which self-assembly of helical structures disrupts the π-π stacking of pyrene and consequently restricts excimer formation in the gel-state, leading to different emission colors for the gel and solution states (Fig. 1A).[5a] Similar behavior to produce two distinct outputs has been observed in a bis(phenylene vinylene)benzothiadiazole derivative that exhibits green and yellow fluorescence depending on its solution or gel state, respectively (Fig. 1B).[5b]

In the context of optically responsive materials, photochromic diarylethenes (DAEs) have received widespread attention due to the robustness of the reversible photoinduced isomerization reactions between the two, spectrally well-resolved, isomers.[7] In this respect, Irie and co-workers reported multicolored photochromic crystals containing mixtures of DAEs (Fig. 1C).[8] Furthermore, the same group reported a single molecule containing three different DAE units that can be selectively isomerized to generate four distinct colored states.[9] Similarly, Branda reported a three-component DAE copolymer in which 8 (2^3) colored states could be achieved (Fig. 1D).[10] In all these examples UV/Vis absorption was used for information readout. This strategy may not always be effective due to the low sensitivity of UV/Vis absorption measurements in combination with the fact that absorption measurements require external circuitry to determine the readout value ($A=\log I_0/I$).[11]

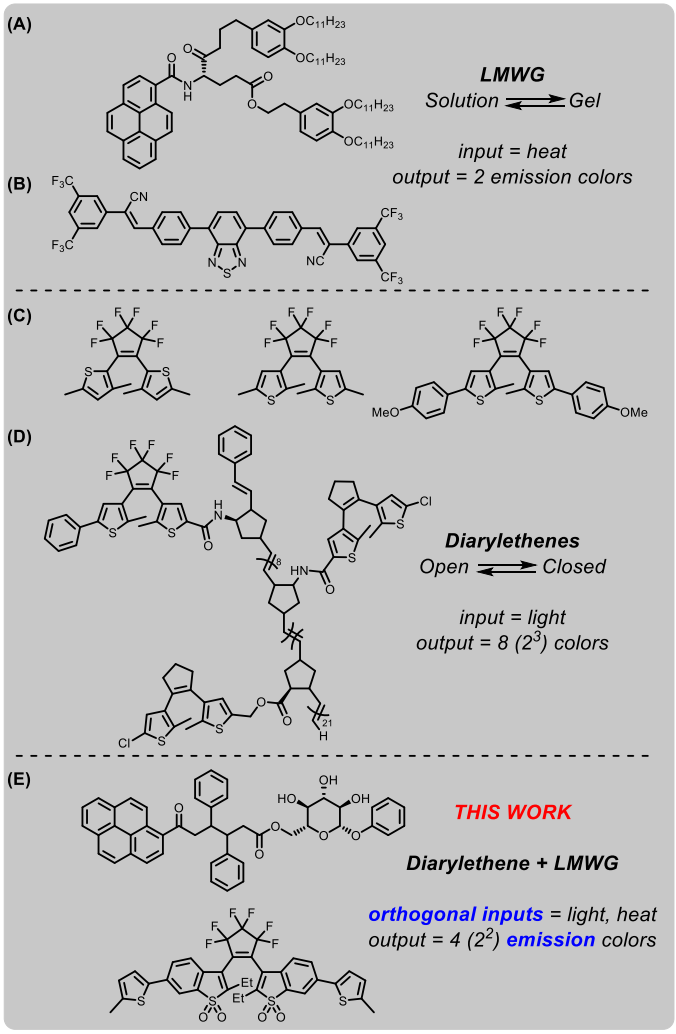

Figure 1. Examples of systems displaying stimuli-responsive color changes based on single and multiple inputs: (A),(B) heat; (C),(D) light; (E) heat and light.

Luminescence mode detection offers much higher sensitivity.[12] In this regard, Kurihara and co-workers reported multicolored fluorescent DAE nanoparticles that could switch among four colored states: white, cyan, orange and dark (although it may be debatable if a non-fluorescent state can be considered as representing an emission color).[13] Similar efforts using light and heat as an input control for tunable/switchable multicolored emission systems has been performed in a variety of systems using nanoparticles,[14] micelles,[15] quantum dots,[16] thin films,[17] and gels.[18] Typically these examples involve two or three-state systems, where a maximum of three emissive states can be achieved as dark states are often involved. In order to exceed this limit, systems capable of generating four distinct emissive states must be developed, preferably where

switching is achieved *via* true orthogonal inputs. Notably, emissive four-state systems have not been reported in multistimuli-responsive materials using photoswitching in conjunction with thermoresponsive gels.

Recently we reported supramolecular systems based on micelles[19] and LMWGs,[20] in combination with mixed fluorophore systems (referred to as "cocktails") that were capable of multi-color emission *via* all-photonic modulation. Such systems involve strategic utilization of energy transfer between chromophores in cocktails consisting of DAEs and fluorescent donor molecules.

Herein, we report the synthesis, and the rheological and photophysical characterization of a pyrene-functionalized oxotriphenylhexanoate (OTHO) gelator and its utilization in a stimuli-responsive multi-color fluorescence system. The pyrene-decorated OTHO gelator shows substantial differences in the emission color in switching between Sol and Gel state. Furthermore, a larger range of emission colors is attainable when a cocktail of the gelator and a fluorescent DAE photoswitch is employed, using heat and light as input triggers. By controlling the Sol-Gel transformation with heat and the isomeric state of the DAE derivative with light (two external stimuli), 4 (2^2) distinct emissive states can be reached. The input triggers are highly orthogonal as the emission from the DAE photoswitch does not change upon gelation or heat exposure and likewise light exposure (for DAE isomerization) does not influence the intrinsic spectral properties of the pyrene fluorophore.

Result and Discussion

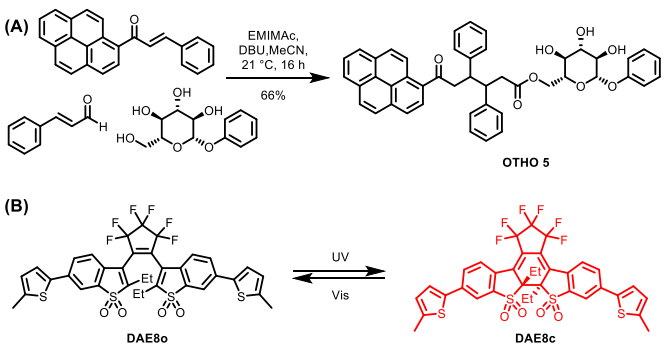

Scheme 1. (A) Three-component synthesis of the OTHO5 gelator. (B) Chemical structure of the open (DAE8o) and closed (DAE8c) isomeric form of the photoswitch.

The chemical structure of the pyrene-based OTHO gelator and photoswitch DAE8 are shown in Scheme 1. DAE8 was synthesized according to the literature procedure.[21] The OTHO gelator was synthesized in an ionic liquid-mediated three-component reaction[22] where the pyrene-containing chalcone, cinnamaldehyde, and phenyl-β-D-glucopyranoside were mixed in the presence of EMIMAc and DBU at room temperature. Following flash chromatography, OTHO5 was isolated in 66% yield (see Supporting Information for full characterization data including ^{1}H, ^{13}C NMR spectra, and HR-MS). The gelating ability of OTHO5 was investigated using the inverted vial method with a range of solvents and solvent mixtures. OTHO5 gelates in toluene, dichlorobenzene, ethyl acetate and in mixtures of toluene and acetonitrile (Table S1 and Figure S1). The minimum gelation concentration of OTHO5 in toluene was 9 mg/mL.

Dynamic shear oscillation experiments were performed to evaluate the rheological properties of the gel. The gel displays typical viscoelastic behavior of a physical gel in the frequency sweep (Figure 2A), where the moduli are largely frequency independent and the storage modulus (G') is approximately one order of magnitude larger than the loss modulus (G''). These properties are characteristic for LMWG and other supramolecular entangled fibrillar systems.[1a, 23] Due to the strongly fluorescent nature of the pyrene gel, confocal laser scanning microscopy (CLSM) was used to gain insight into the structure of the gel. The CLSM images confirm the presence of a highly entangled fibrillar network in the gel, with the diameter of the fibers in the order of 1 µm (Figure 2B).

The fluorescent properties of OTHO5 were investigated in solution and in the gel phase (Figure 1). In toluene at low concentrations (10^{-5} M), OTHO5 exhibits monomer-like pyrene emission (Figure 2C and 2D) with a quantum yield of 0.26. At higher concentrations (> 10^{-3} M), OTHO5 begins to aggregate and assembly into fibrils, where a moderate component belonging to the excimer emission is present. In the gel phase, OTHO5 shows a broad emission band with mixed components from excimers and other restricted conformations present in the gel. The fluorescence lifetimes of OTHO5 gel in toluene were determined by time-correlated single photon counting. The lifetimes of OTHO5 monomer and excimer were substantially shorter than those of pyrene solutions (see SI, Figures S8 and S9).[24]

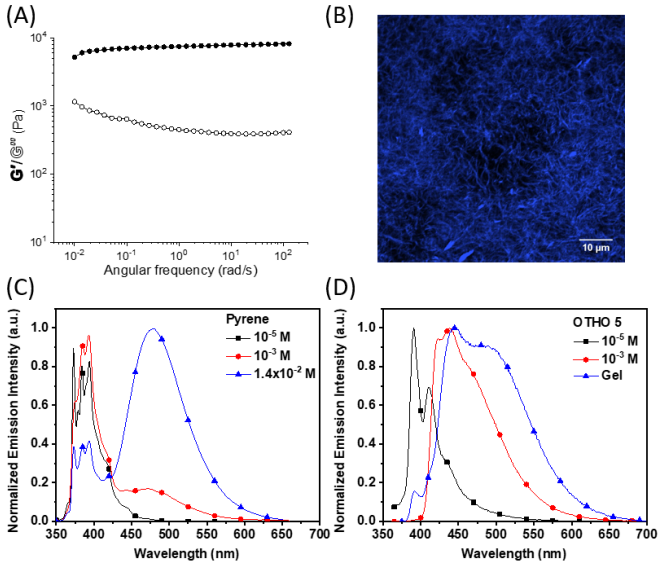

Figure 2. (A) Frequency sweep of OTHO5 gel in toluene 10 mg/mL, storage modulus (●) and loss modulus (○), 0.5% strain, 20 °C. (B) Confocal laser scanning microscopy image of OTHO5 gel, 405 nm laser excitation. (C) Emission spectra of pyrene in toluene solution, λ_{ex} = 340 nm. (D) Emission spectra of OTHO5 in toluene solution and gel, λ_{ex} = 370 nm.

Interestingly, the risetime observed with pyrene solution excimer emission is not present in the gel, indicating that excimer formation is no longer a dynamic process and the pyrene units are confined in the rigid environment of the gel fibers.[25]

Gelation of OTHO5 occurs rapidly in toluene upon cooling to room temperature. In acetonitrile, however, it remains in solution or in a partial gel state. In the case of toluene and acetonitrile mixtures, there are no observable changes in gelation at higher toluene/acetonitrile ratio (9:1), but with increasing acetonitrile, the gel forms slowly upon cooling, while sonication accelerates the gelation process and improves sample uniformity. When the acetonitrile ratio is more than 50%, OTHO5 does not fully gelate, but instead dissolves or forms a partial gel even after sonication. Figure 3A shows OTHO5 in the 2:1 ratio of toluene/acetonitrile. Here, it remains temporarily in solution state at room temperature (left) but will gelate immediately when sonication is applied (right). Under UV light irradiation the emission color is dramatically different in solution and in the gel (Figure 3B). In Figure 3C, it can be clearly seen that OTHO5 (10 mg/mL) in the sol state presents excimer emission centered at 525 nm. However, when OTHO5 forms a gel, the excimer emission intensity is less pronounced. This observation is likely due to self-assembly into initial 1D fibrillar structures and a subsequent breakage of the π-π stacking of the pyrene molecules.[5a, 26] Thus, the excimer emission is much more pronounced in solution compared to the gel state. Mapping these emission spectra in the CIE diagram, the coordinates for the solution and the gel are clearly distinct (Figure 3D).

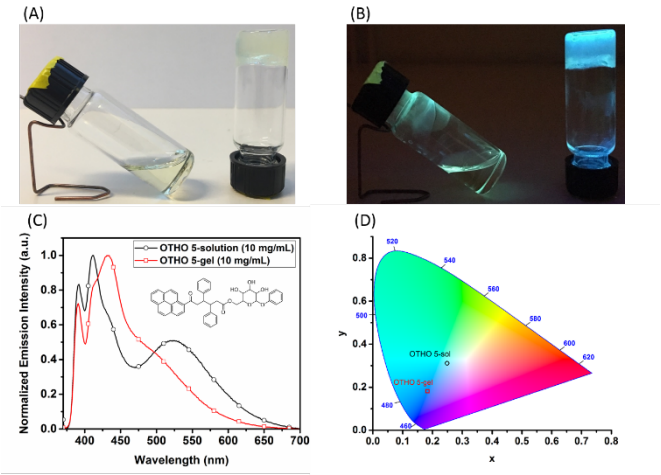

Figure 3. (A) Photos of OTHO5 gel under ambient light. Left: After heating (sol). Right: Before heating (gel). (B) Photos of OTHO5 gel under 365 nm light. Left: After heating (sol). Right: Before heating (gel). (C) Emission spectra of OTHO5 in solution and gel, λ_{ex} = 370 nm. (D) CIE diagram of OTHO5 in solution and gel. The concentration of OTHO5 is 10 mg/mL, toluene/acetonitrile = 2:1.

Having found optimal conditions for a heat controlled Sol-Gel transition, corresponding to two signals for optical read-out, we opted for a system containing an additional fluorophore with tunable spectral properties. We were particularly interested in devising a bi-component system where the input triggers for the two fluorophores are highly orthogonal, implying that the respective fluorophore could be addressed with a high degree of selectivity. Accordingly, OTHO5 gelator (10 mg/mL, 1.4×10^{-2} M) and DAE8 (10^{-4} M) were dissolved in toluene/acetonitrile (2:1). By defining the two input triggers as heat (controlling the solution-gel transformation, affecting only the pyrene emission in OTHO5) and UV exposure (isomerizing DAE8 to the closed fluorescent isomeric form without affecting the intrinsic pyrene emission in OTHO5) there will be 4 (2^2) distinct states generated. These are OTHO5-Sol/DAE8o, OTHO5-Gel/DAE8o, OTHO5-Sol/DAE8c, and OTHO5-Gel/DAE8c. Figure 4A shows the overall emission spectra of OTHO5/DAE8 in these four situations. With the DAE in the open form (no UV exposure), the OTHO5/DAE8o mixture exhibits blue emission in gel state and green emission in solution state. However, when exposed to UV light DAE8 isomerizes from the open form to the closed form and emits in the red region (See Figure S5 for the emission spectrum of DAE8c). Thus, OTHO5/DAE8c displays pink emission in gel state and orange emission in solution state.[27] Mapping these emission profiles into the CIE diagram (Figure 4B) clearly shows the four distinct emissive states that can be achieved with these input triggers (heat and UV-light). It is interesting to note that virtually perfect white light is being generated upon isomerizing the DAE photoswitch between the open and the closed isomer in the sol-state (actual CIE coordinate (0.33, 0.32) compared to (0.33, 0.33) for perfect white light).

To test whether the emission from DAE8c was affected by switching between the solution and gel state, the emission spectra were recorded in the presence of an OTHO gelator lacking the pyrene unit. The absorption and emission profiles were unchanged between solution and gel state (Figure S6 and S7, emission CIE coordinates: 0.644, 0.356, Φ_f = 0.25), demonstrating that the multi-colored emission system employs truly orthogonal input triggers.

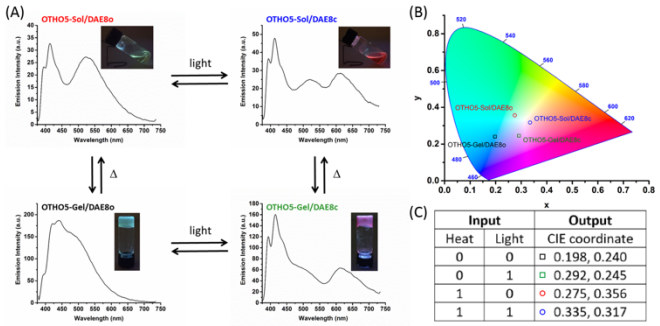

Input		Output
Heat	Light	CIE coordinate
0	0	0.198, 0.240
0	1	0.292, 0.245
1	0	0.275, 0.356
1	1	0.335, 0.317

Figure 4. (A) Multicolored emission triggered by solution-gel transformation (heat) and UV irradiation for isomerization of DAE8o to DAE8c (λ=380 nm). (B) Mapping the CIE coordinates of the four emission spectra in the CIE diagram (C) CIE coordinates of OTHO5/DAE8 with different combinations of the input triggers. The concentration of OTHO5 is 10 mg/mL, DAE8 is 10^{-4} M, toluene/acetonitrile = 2:1. The spectra were recorded at room temperature with λ_{ex} = 370 nm.

Conclusions

In summary, a pyrene-modified OTHO that gelates in a range of solvents has been devised. It manifests different degrees of pyrene monomer and excimer emission in solution and gel state owing to the self-assembly and disruption of the π-π stacking. Furthermore, a multi-color readout system has been realized by combining the photophysical/spectral changes that accompany the Sol-Gel transformation with a fluorescent DAE photoswitch. The use of two highly orthogonal inputs, heat and light, enables the bi-component OTHO/DAE cocktail to generate four distinct emissive states. This is a powerful approach to multi-wavelength readout systems, offering a situation where substantially more information can be encoded, compared to the binary on-off situations displayed by systems built on single fluorophore emission. Increasing the number of inputs to three stimuli could potentially generate 8 (2^3) distinct output states,[28] although this becomes increasingly challenging with mixed chromophore systems if orthogonal switching is desired. Moreover, accessing a larger region of the CIE space would undoubtedly add to the appeal, and could imply the inclusion of a green emitter. Efforts along these lines are presently being undertaken in our laboratory.

Acknowledgements

We gratefully acknowledge the Swedish Research council (VR and Formas) for funding and Carl-Tryggers foundation and the Swedish Energy Agency for providing postdoc fellowships for C.-W.H. and M.D.J., respectively. Chalmers Excellence Initiative in Nano- science and Nanotechnology, Adlerbert Research Foundation and Wilhelm and Martina Lundgren Research Foundation are also acknowledged for funding. This work was performed in part at the Chalmers Material Analysis Laboratory, CMAL.

Conflicts of interest

There are no conflicts to declare.

References

[1] a) P. Terech, R. G. Weiss, *Chem. Rev.* **1997**, *97*, 3133-3160; b) J. W. Steed, *Chem. Commun.* **2011**, *47*, 1379-1383.

[2] a) C. D. Jones, J. W. Steed, *Chem. Soc. Rev.* **2016**, *45*, 6546-6596; b) E. R. Draper, D. J. Adams, *Chem. Commun.* **2016**, *52*, 8196-8206; c) Z. Sun, Q. Huang, T. He, Z. Li, Y. Zhang, L. Yi, *ChemPhysChem* **2014**, *15*, 2421-2430; d) S. Yagai, A. Kitamura, *Chem. Soc. Rev.* **2008**, *37*, 1520-1529; e) Z. Ding, Y. Ma, H. Shang, H. Zhang, S. Jiang, *Chem. Eur. J.* **2019**, *25*, 315-322; f) X. Wang, Z. Ding, Y. Ma, Y. Zhang, H. Shang, S. Jiang, *Soft Matter* **2019**, *15*, 1658-1665.

[3] a) S. S. Babu, V. K. Praveen, A. Ajayaghosh, *Chem. Rev.* **2014**, *114*, 1973-2129; b) S. Wang, W. Shen, Y. Feng, H. Tian, *Chem. Commun.* **2006**, 1497-1499; c) S. Xiao, Y. Zou, M. Yu, T. Yi, Y. Zhou, F. Li, C. Huang, *Chem. Commun.* **2007**, 4758-4760.

[4] a) B.-K. An, D.-S. Lee, J.-S. Lee, Y.-S. Park, H.-S. Song, S. Y. Park, *J. Am. Chem. Soc.* **2004**, *126*, 10232-10233; b) B.-K. An, J. Gierschner, S. Y. Park, *Acc. Chem. Res.* **2012**, *45*, 544-554; c) Z. Zhao, J. W. Y. Lam, B. Z. Tang, *Soft Matter* **2013**, *9*, 4564-4579; d) Y. Hong, J. W. Y. Lam, B. Z. Tang, *Chem. Soc. Rev.* **2011**, *40*, 5361-5388.

[5] a) Y. Kamikawa, T. Kato, *Langmuir* **2007**, *23*, 274-278; b) C. Dou, D. Chen, J. Iqbal, Y. Yuan, H. Zhang, Y. Wang, *Langmuir* **2011**, *27*, 6323-6329; c) N. Yan, Z. Xu, K. K. Diehn, S. R. Raghavan, Y. Fang, R. G. Weiss, *Langmuir* **2013**, *29*, 793-805; d) C.-B. Huang, L.-J. Chen, J. Huang, L. Xu, *RSC Adv.* **2014**, *4*, 19538-19549.

[6] a) T. Shu, J. Wu, M. Lu, L. Chen, T. Yi, F. Li, C. Huang, *J. Mater. Chem.* **2008**, *18*, 886-893; b) A. Das, S. Ghosh, *Angew. Chem. Int. Ed.* **2014**, *53*, 2038-2054; c) M. A. Castilla, B. Dietrich, J. D. Adams, *Gels* **2018**, *4*.

[7] a) M. Irie, T. Fukaminato, K. Matsuda, S. Kobatake, *Chem. Rev.* **2014**, *114*, 12174-12277; b) S.-Z. Pu, Q. Sun, C.-B. Fan, R.-J. Wang, G. Liu, *J. Mater. Chem. C* **2016**, *4*, 3075-3093; c) T. Mosciatti, M. G. del Rosso, M. Herder, J. Frisch, N. Koch, S. Hecht, E. Orgiu, P. Samorì, *Adv. Mater.* **2016**, *28*, 6606-6611.

[8] a) M. Morimoto, S. Kobatake, M. Irie, *Adv. Mater.* **2002**, *14*, 1027-1029; b) M. Morimoto, S. Kobatake, M. Irie, *J. Am. Chem. Soc.* **2003**, *125*, 11080-11087.

[9] K. Higashiguchi, K. Matsuda, N. Tanifuji, M. Irie, *J. Am. Chem. Soc.* **2005**, *127*, 8922-8923.

[10] T. J. Wigglesworth, N. R. Branda, *Chem. Mater.* **2005**, *17*, 5473-5480.

[11] A. J. Myles, N. R. Branda, *Adv. Funct. Mater.* **2002**, *12*, 167-173.

[12] T. B. Norsten, N. R. Branda, *J. Am. Chem. Soc.* **2001**, *123*, 1784-1785.

[13] S. Ishida, T. Fukaminato, D. Kitagawa, S. Kobatake, S. Kim, T. Ogata, S. Kurihara, *Chem. Commun.* **2017**, *53*, 8268-8271.

[14] a) J. Chen, P. Zhang, G. Fang, P. Yi, F. Zeng, S. Wu, *J. Phys. Chem. B* **2012**, *116*, 4354-4362; b) L. Zhu, W. Wu, M.-Q. Zhu, J. J. Han, J. K. Hurst, A. D. Q. Li, *J. Am. Chem. Soc.* **2007**, *129*, 3524-3526; c) S. Ishida, T. Fukaminato, S. Kim, T. Ogata, S. Kurihara, *Chem. Lett.* **2017**, *46*, 1182-1185; d) K. Watanabe, H. Hayasaka, T. Miyashita, K. Ueda, K. Akagi, *Adv. Funct. Mater.* **2015**, *25*, 2794-2806; e) S. Kim, S.-J. Yoon, S. Y. Park, *J. Am. Chem. Soc.* **2012**, *134*, 12091-12097; f) J. Bu, K. Watanabe, H. Hayasaka, K. Akagi, *Nat. Commun* **2014**, *5*, 3799.

[15] C. Li, Y. Zhang, J. Hu, J. Cheng, S. Liu, *Angew. Chem. Int. Ed.* **2010**, *49*, 5120-5124.

[16] a) S. A. Díaz, L. Giordano, T. M. Jovin, E. A. Jares-Erijman, *Nano Lett.* **2012**, *12*, 3537-3544; b) S. A. Díaz, F. Gillanders, K. Susumu, E. Oh, I. L. Medintz, T. M. Jovin, *Chem. Eur. J.* **2017**, *23*, 263-267.

[17] a) H.-J. Kim, D. R. Whang, J. Gierschner, C. H. Lee, S. Y. Park, *Angew. Chem. Int. Ed.* **2015**, *54*, 4330-4333; b) W. Tian, J. Zhang, J. Yu, J. Wu, J. Zhang, J. He, F. Wang, *Adv. Funct. Mater.* **2018**, *28*, 1703548.

[18] a) J. W. Chung, S.-J. Yoon, S.-J. Lim, B.-K. An, S. Y. Park, *Angew. Chem. Int. Ed.* **2009**, *48*, 7030-7034; b) A. Kishimura, T. Yamashita, T. Aida, *J. Am. Chem. Soc.* **2005**, *127*, 179-183; c) D. Kim, J. E. Kwon, S. Y. Park, *Adv. Funct. Mater.* **2018**, *28*, 1706213.

[19] M. Bälter, S. Li, M. Morimoto, S. Tang, J. Hernando, G. Guirado, M. Irie, F. M. Raymo, J. Andréasson, *Chem. Sci.* **2016**, *7*, 5867-5871.

[20] C.-W. Hsu, C. Sauvée, H. Sundén, J. Andréasson, *Chem. Sci.* **2018**, *9*, 8019-8023.

[21] K. Uno, H. Niikura, M. Morimoto, Y. Ishibashi, H. Miyasaka, M. Irie, *J. Am. Chem. Soc.* **2011**, *133*, 13558-13564.

[22] a) A. Axelsson, L. Ta, H. Sundén, *Eur. J. Org. Chem.* **2016**, 3339-3343; b) L. Ta , A. Axelsson , J. Bijl, M. Haukka, H. Sundén, *Chem. Eur. J.* **2014**, *20*, 13889-13893; c) A. Axelsson, L. Ta, H. Sundén,

Catalysts **2015**, *5*, 2052-2067; d) C. Sauvée, A. Ström, M. Haukka, H. Sundén, *Chem. Eur. J.* **2018**, *24*, 8071-8075.
[23] P. Terech, D. Pasquier, V. Bordas, C. Rossat, *Langmuir* **2000**, *16*, 4485-4494.
[24] J. B. Birks, D. J. Dyson, I. H. Munro, H. Flowers Brian, *Proc. R. Soc. London, Ser. A* **1963**, *275*, 575-588.
[25] a) J. Matsui, M. Mitsuishi, T. Miyashita, *J. Phys. Chem. B* **2002**, *106*, 2468-2473; b) T. Yamazaki, N. Tamai, I. Yamazaki, *Chem. Phys. Lett.* **1986**, *124*, 326-330.
[26] a) J. Lee, H. Jung, H. Shin, J. Kim, D. Yokoyama, H. Nishimura, A. Wakamiya, J. Park, *J. Mater. Chem. C* **2016**, *4*, 2784-2792; b) C. Wang, Z. Wang, D. Zhang, D. Zhu, *Chem. Phys. Lett.* **2006**, *428*, 130-133.
[27] Energy transfer from pyrene to DAE8 in both isomeric forms is also contributing to the spectral changes. The mechanism of the energy transfer process is mainly "trivial": emission from pyrene followed by reabsorption of DAE8. FRET is not expected to be efficient considering the low concentration of DAE8.
[28] Figure S10 demonstrates that eight distinct CIE coordinates can be accomplished with three different stimuli. However, those CIE coordinates are very close to each other due to the inefficient FRET (the emission of pyrene is not overlapping with the absorption of DAEs and the concentration of pyrene is much higher than DAEs).